

OPEN ACCESS

Synthesis and Optical Investigations of the Guest-Host Nanostructures Alumina-SiC and Alumina- In_2O_3

To cite this article: A Bouifoulen *et al* 2011 *J. Phys.: Conf. Ser.* **289** 012001

View the [article online](#) for updates and enhancements.

You may also like

- [Fe&Fe₂O₃ Dual-Decorated on N-Doped Porous Carbon for Oxygen Reduction Reaction](#)
Hui-Juan Zhang, Ye He, Bo Chen et al.
- [Tunable bandgap energy of fluorinated nanocrystals for flash memory applications produced by low-damage plasma treatment](#)
Chi-Hsien Huang, Chih-Ting Lin, Jer-Chyi Wang et al.
- [Mechanistic understanding of the charge carrier trapping in CsPbCl₃ perovskite nanocrystals](#)
Ji Li, Yue Hu, Xuemin Hou et al.

ECS
The
Electrochemical
Society
Advancing solid state &
electrochemical science & technology

DISCOVER
how sustainability
intersects with
electrochemistry & solid
state science research

Synthesis and Optical Investigations of the Guest-Host Nanostructures Alumina-SiC and Alumina-In₂O₃

A Bouifoulen^{1,2}, A Kassiba¹, A Outzourhit², M Edely¹, M Makowska-Janusik³, J Szade⁴, A Oueriagli²

¹ Laboratoire de Physique de l'Etat Condensé, UMR-CNRS 6087, Institut de recherche IRIM2F-FR-CNRS 2575-Université du Maine, Avenue Olivier Messiaen, 72085 Le Mans Cedex 9, France

² Laboratoire de Physique du Solide et Couches Minces, Faculté des Sciences Semlalia, Université Cadi Ayyad, B. P. 2390, Marrakech 40000, Maroc

³ Institute of Physics, Al. Armii.Krajowej, 13/15, J. Dlugosz University, 42-200 Czestochowa, Poland

⁴ A.Chelkowski Institute of Physics - University Śląski in Katowice - 40-219 Katowice, Poland

Email: kassiba@univ-lemans.fr

Abstract. Several strategies were developed to synthesise two classes of nanostructured thin films with nanocrystals of SiC (nc-SiC) or In₂O₃ (nc-In₂O₃) confined in alumina. The syntheses were performed by using Rf-sputtering and co-pulverisation process of the suitable reactants. Thus, Al₂O₃/nc-SiC and Al₂O₃/nc-In₂O₃ composite thin films were obtained and their structural and optical features analyzed respectively by XRD, XPS and UV-VIS absorption. The deposition conditions and the post-synthesis treatments were optimized in order to improve the crystalline character of confined nanocrystals. The optical properties were compared in the range 200 nm-1200 nm for bare alumina films or nanostructured ones with the semiconducting nanocrystals. The direct and indirect band gaps were evaluated and discussed with regard to the stoichiometry and morphologies of the nanocomposite films

1. Introduction

Nanostructured films composed by semi-conducting nanocrystals confined in background host matrices are attractive architectures with regard to expected original electronic and optical behaviours. The key parameters which monitor the quality of the nanostructure consist in narrow size and shape distributions of the nanocrystals in the matrix as well as their homogeneous crystalline order. Among the considered materials, silicon carbide nanocrystalline (SiC) is a wide bandgap semiconductor with particular characteristics such as high breakdown field strength, high thermal conductivity, and high saturation drift velocity [1]. These excellent physical properties make SiC a promising semiconductor material for the fabrication of electronic devices [2]. Moreover, as an important wide band gap semiconductor, cubic silicon carbide (β -SiC) nanostructures would be favourable for applications in high temperature, high power, and high frequency nanoelectronic devices [3]. From another hand, besides the interest in applications in optoelectronics, In₂O₃ nanostructures have also a key role from a fundamental to applications in several areas such as solar cells, sensors or flat panel displays [4]. As main characteristics of indium oxide, the direct band gap is around 3.75 eV and the indirect bandgap at about 2.61 eV [5] lead to high optical transparency in the visible light region [6].

In another respect, alumina (Al₂O₃) is the most important dielectric material suitable for optical coatings in large spectral region [7]. Therefore, it is considered to be the most promising candidates to

realize composites with improved optical properties taking benefit from SiC and In₂O₃ nanocrystals whose the size and crystalline polytypes can modulate the band gap in a large extent.

For the practical achievement of the synthesis, although DC magnetron sputtering is more preferred for industrial applications, rf-sputtering is more suited for our purpose. The experimental versatility allows modulating the structural and optical properties of alumina-SiC and alumina-In₂O₃ through the nature of substrates, deposition conditions such as temperature of substrate during deposition, annealing and also the electrical power of the deposition process.

Thus, this work is dedicated to realize composites such as alumina-SiC and alumina-In₂O₃ films deposited on (100) silicon or borosilicate (BK7) substrates at different temperatures and to investigate the variations of structural and optical properties. The morphology, microstructure and the composition of alumina-SiC and alumina-In₂O₃ films were characterized by methods such as XRD and XPS. In addition, optical transmittance spectra were compared between the as-deposited and post-annealed composites films associating alumina and SiC or In₂O₃ nanocrystals. The evaluation of direct and indirect band gap was performed as function of the compositions of nanostructured films.

2. Experimental

2.1. Materials

Alumina-SiC and alumina-In₂O₃ thin films were deposited onto crystalline (100) silicon wafer and borosilicate glass substrates by rf-sputtering method using co-deposition from Al₂O₃ target and pellets of SiC or In₂O₃. The rf sputtering power was varied in the range 50 – 100 Watt. The SiC pellets were hot-pressed while the In₂O₃ pellets were sintered at 1300°C [8]. Typically, the base vacuum was about 1.4 10⁻⁶ mbar, and the pressure was stabilized at about 10.98 10⁻² mbar during the deposition process with the flow rate of argon about 100 sccm. After cleaning, the float substrates were placed in the vacuum chamber. The substrates were heated from room temperature (20°C) to 600 °C. The film thickness of about 310 nm was achieved. In this study, only the substrate temperature was varied, while all deposition times presented here were 60 min and all other parameters were fixed.

2.2. Methods

The film thickness was measured using an interferometer (FilmeTrics Model 205-0070). The phase composition and structure of the samples was determined by X-ray diffraction using a Philips X-pert diffractometer with a Cu-K α radiation. Optical transmittance spectra of the film structure were measured with a UV-VIS-NIR scanning spectrophotometer (DH-2000-BAL). High resolution transmission electron microscopy (TEM) images were obtained on the composite samples based on SiC and Al₂O₃. XPS investigations were performed with a Mg K α X-ray excitation source (1253.6 eV). The residual pressure in the analysis chamber was maintained below 10⁻⁹ torr during data acquisition. The various XPS spectra with high resolution were recorded for the elements Si 2p, C 1s and Al 2p.

3. Results and discussion

3.1. Structural and morphology features

Figure 1(a) shows XRD patterns of as-deposited and 800°C annealed films. The annealing is performed in a furnace under Ar atmosphere during 3 hours. The high temperature annealing (800°C) favours the development of a large diffraction background from of small (111) SiC peak at about 2 θ =33.6°. Previous experimental results [9] showed that this structure appears when the annealing is made at 900°C. Figure 1(b) reports the XRD pattern of alumina-In₂O₃ samples which were deposited onto silicon substrate and prepared at temperature of substrates at about 20°C, 250°C and 400°C. It can be seen that the main growth directions are (2 1 1), (2 2 2), (4 0 0) and (4 4 0), which are related to the cubic structure of In₂O₃ [10]. Under the same conditions, depositions of these samples were also made on a borosilicate glass. This procedure allow to resolve better the main diffraction line related for the In₂O₃ main phase (Figure 1(c)). As-deposited films at RT and the one with the substrate temperature fixed at 250°C exhibit amorphous features. The films were crystallized only for the temperature as high as 400°C leading to a XRD (222) peak enhancement. Finally, None of the diffraction patterns bring the mark of any characteristic peaks of alumina. This is indicative of amorphous nature of the alumina matrix.

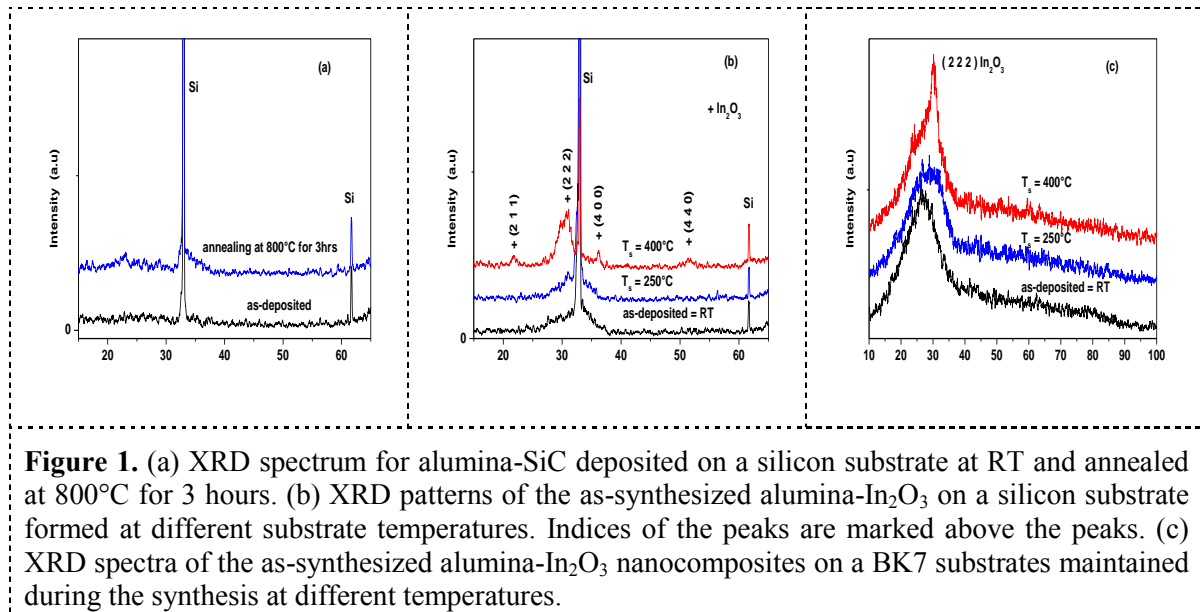


Figure 1. (a) XRD spectrum for alumina-SiC deposited on a silicon substrate at RT and annealed at 800°C for 3 hours. (b) XRD patterns of the as-synthesized alumina-In₂O₃ on a silicon substrate formed at different substrate temperatures. Indices of the peaks are marked above the peaks. (c) XRD spectra of the as-synthesized alumina-In₂O₃ nanocomposites on a BK7 substrates maintained during the synthesis at different temperatures.

The XPS experiments give valuable information on the composition of the films. XPS spectra were recorded and deconvoluted for precise identification of the involved chemical species. Figure 2(a) shows the XPS spectra of Si 2p core level peak. The deconvolution of this spectrum reveals two components. The one located at a binding energy of 103.17 eV is associated to environments such as Si-O₂ [11]. The second contribution located at energy about 99.60 eV is assigned to bonding which can be attributed to Si-C [12]. Such involved bonding with silicon seems sound with respect to the coexistence of SiC clusters and the expected formation of SiO₂ during the co-pulverization of Alumina.

The spectrum of the C 1s level in figure 2(b) seems to reveal three bonding features. The peak position located at a binding energy of 284.81 eV corresponds to C-C [11] bonding. The second contribution located around the energy of 283.49 eV can be assigned to C-Si [11] bond while the features at the binding energy of 286.45 eV correspond to C-H bond [13]. It is worth noting that, the involved hydrogen bonding occurs from the composition of the SiC pellets made from powders which contain hydrogen due to the used synthesis process [14].

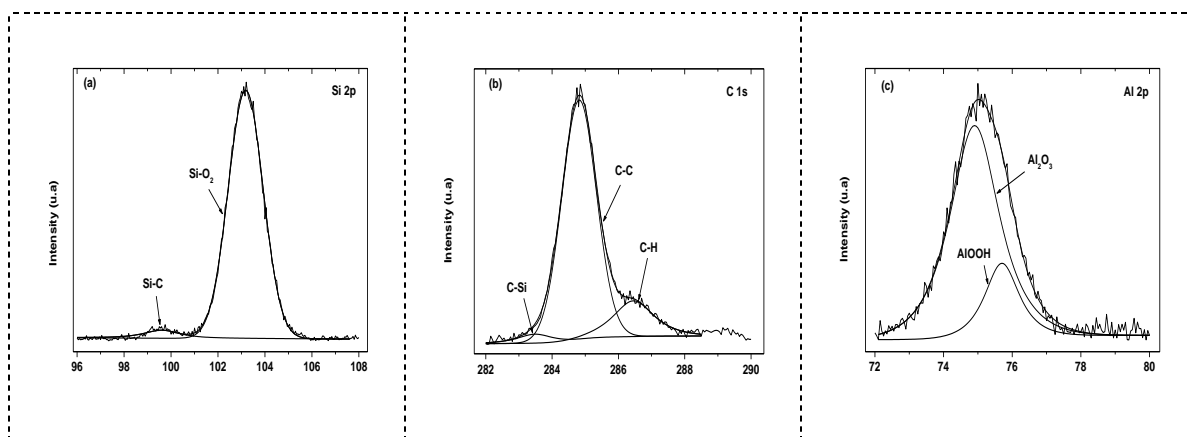


Figure 2. (a) Typical deconvoluted XPS spectrum of Si 2p energy region for the alumina-SiC. (b) Typical deconvoluted XPS spectrum of C 1s energy region for the alumina-SiC. And (c) Typical deconvoluted XPS spectrum of Al 2p energy region for the alumina-SiC.

Figure 2(c) presents the XPS spectra of the Al 2p core level peak and its decomposition reveals two superimposed components with a small difference in the binding energy. Both are most likely

associated to alumina [15]. The low intensity line at about 75.7 eV may be related to a non-stoichiometric compound.

3.2. Optical features

The transparency of the synthesized films for all temperatures exhibits similar features shown in Figure 3(a,b). At the opposite of SiC based composites, the more pronounced optical effects were obtained after the incorporation of In_2O_3 . Indeed at given wavelength about 650 nm, the transmission percent of alumina- In_2O_3 films changes from 84% (RT deposited), to 89% for deposition with the substrate at (250°C) and to 93% for substrate temperature about (400°C). The ripples in the spectrum resulted from the interference fringes due to suitable film thickness for resolving interferences effects [16].

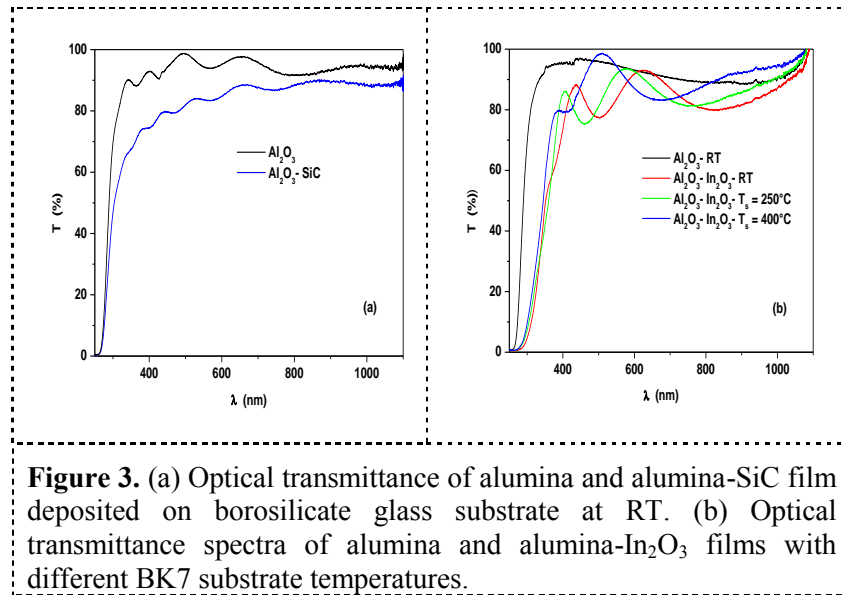


Figure 3. (a) Optical transmittance of alumina and alumina-SiC film deposited on borosilicate glass substrate at RT. (b) Optical transmittance spectra of alumina and alumina- In_2O_3 films with different BK7 substrate temperatures.

The type of the optical transitions, whether direct or indirect, can be determined by studying the dependence of the absorption coefficient $\alpha = [\ln(1/T)/d]$, as function of the photon energy ($h\nu$) and the thickness (d) of the films. For direct/indirect optical transition between presumably parabolic bands, the relevant optical band gaps parameters can be deduced as follows [17].

$$(\alpha \cdot h\nu)^n = A \cdot (h\nu - E_g) \quad (1)$$

Where A is a constant and E_g is the optical band gap. The direct and indirect bandgaps of the composites films may roughly be estimated by plotting $(\alpha \cdot h\nu)^n$ versus $h\nu$ ($n=2$ for allowed direct and $n=1/2$ for allowed indirect optical transitions). By extrapolating the linear region of the plot toward low energies [18], we may deduce the optical band-gaps. Figure 4(a,b) and figure 5(a,b) represents these plots for the alumina (RT), alumina-SiC (RT) and alumina- In_2O_3 (RT, 250, 400°C). Table 1 summarizes all bandgaps obtained by extrapolating the linear parts of the $(\alpha h\nu)^n$ versus $h\nu$ plots.

Table 1. Variation of the direct and indirect band-gap of nanocomposite films.

n	Al_2O_3	Al_2O_3 -SiC	Al_2O_3 - In_2O_3		
			RT	250°C	400°C
1/2 (eV) (indirect)	4.04	3.94	3.09	3.07	3.20
2 (eV) (direct)	4.51	4.48	3.92	4.05	4.09

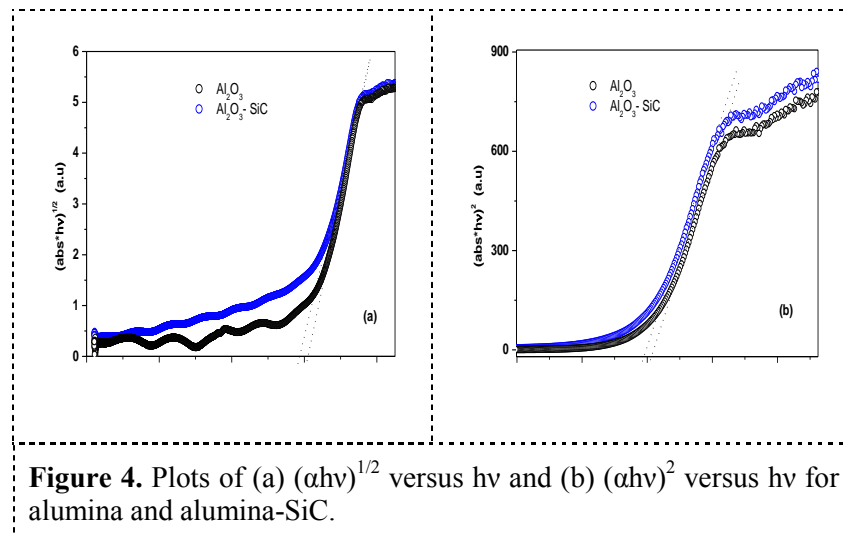


Figure 4. Plots of (a) $(\alpha h\nu)^{1/2}$ versus $h\nu$ and (b) $(\alpha h\nu)^2$ versus $h\nu$ for alumina and alumina-SiC.

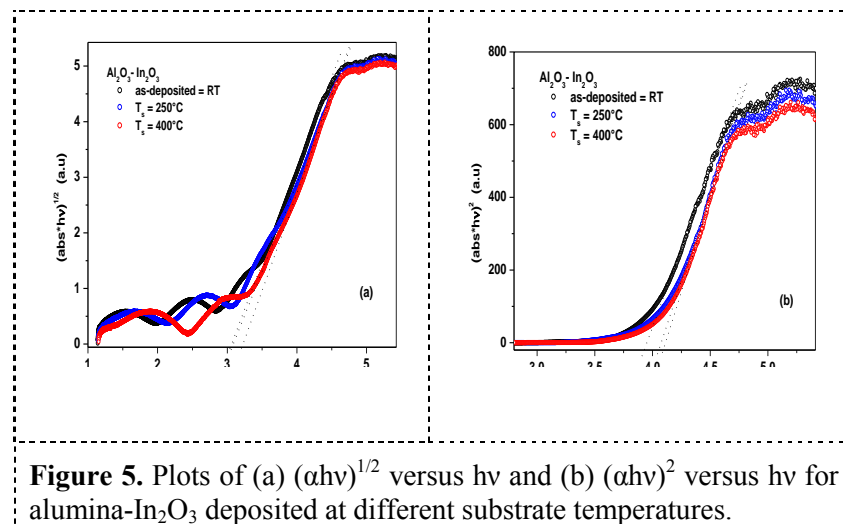


Figure 5. Plots of (a) $(\alpha h\nu)^{1/2}$ versus $h\nu$ and (b) $(\alpha h\nu)^2$ versus $h\nu$ for alumina-In₂O₃ deposited at different substrate temperatures.

The obtained band gap, direct and indirect, seem relevant to monitor the composition of the film alumina-nanocrystals.

The optical properties traduce the change in the film composition through the modification of the caractéristiques optical band-gaps. The effects are more importnat on the alumina-In₂O₃ compared to composites with SiC.

4. Conclusions

Innovative guest-host nanostructures can be realized from alumina as host matrix and nanocrystals incorporated in the amorphous media. Two main wide band gap semiconductors (SiC, In₂O₃) were used because their gap can be finely tuned as function of nanocrysal dimensions and their cristalline polytypes. The XRD experiments showed that the crystallinity of alumina-In₂O₃ nanocomposites was improved by using appropriate substrates maintained at temperatures between RT and 400°C. From optical aspects, high quality films with a transmittance 93% were obtained and the allowed-indirect and allowed-direct optical bandgap were found to vary respectively from 3.07 to 3.20 eV and from 3.92 to 4.09 eV, depending on the temperature of the substrates. The effects of In₂O₃ incorpotaion are more important on optical behavior compared to composites based on SiC. The carried out synthesis procedures are currently under development to improve the film quality, cristalline features and morphologies.

Acknowledgements

A part of the work was realized under the France-Morocco cooperation program VOLUBILIS with the financial support from the “Comité inter-universitaire Franco-Marocain”.

References

- [1] Kang B C et al. *Thin Solid Films* 464-465 (2004) 215-219
- [2] Fisher A, Schroter B, Richter W, *Appl. Phys. Lett.* 66 (23) 1995
- [3] Li J C, Lee C S, Lee S T, *Chem. Phys. Lett.* 355 (2002)
- [4] Chen et al. *J. Phys. Chem. C*, Vol. 111, No. 49, 2007
- [5] Mazzerà M et al. *Nanotechnology* 18 (2007) 355707
- [6] Mohan Babu P, *J. Opt. Adv. Mat.* Vol. 6, No. 1, March 2004, p. 205 – 210
- [7] Zhang F et al. *Applied Surface Science* 254 (2008) 3045–3048
- [8] Xu H, Yu A, *Materials Letters* 61 (2007) 4043-4045
- [9] Yoon D H and Suh S J, *J. Korean Phy Soc*, Vol. 42, February 2003, pp. S943-S946
- [10] Gheidari A M et al. *Materials Science and Engineering B* 136 (2007) 37-40
- [11] Santoni A, Frycek R, Castrucci P, Scarselli M, Cres M D, *Surf. Sci.* 582 (2005) 125
- [12] Shimoda K, Park J –S, Hinoki T and Kohyama A, *Appl. Surf. Sci.* 253 (2007) 9450
- [13] Dikov Y P, Ivanov A V, Wlotzka F, M Galimov E, Wanke G, *Solar System Research* 36, 1(2002)1 and references therein
- [14] Bouclé J, Kassiba A, Makowska-Janusik M, Herlin-Boime N, Reynaud C, Desert A, Emery J, Bulou A, Sanetra J, Pud A A, and Kodjikian S, *Phys. Rev. B* 74 (2006) 205417
- [15] NIST standard XPS reference database 20 version 3.5 (2003)
- [16] Lin H, Kumon S, Yoko T, Kozuka H, *Thin Solid films* 1998, 315, 266–272
- [17] K Subba Ramaiah et al. *Semicond. Sci. Technol.* 15 (2000) 676–683
- [18] Novkkovski N and Tanusevski A, *Semicond. Sci. Technol.* 23 (2008) 095012